Self-organization, shape transition, and stability of epitaxially strained islands

Y. W. Zhang*
Institute of Materials Research and Engineering, National University of Singapore, Singapore, 119260
(Received 27 September 1999)

Three-dimensional computer simulations are carried out to investigate the self-organization, shape transition, and stability of epitaxially strained islands during controlled annealing. In the simulations, the strain energy density, surface energy density, and surface energy anisotropy are taken into account. It is found that the phenomena of ripening or nonripening, strong self-organization or weak self-organization, and shape transition or nonshape transition of the island array can be obtained with only slight changes in the surface energy anisotropy. With these simulation results, the inconsistencies that exist in the experimental results are discussed.

INTRODUCTION

Strain-induced self organization of epitaxial islands has drawn considerable attention due to potential application in the fabrication of optoelectronic and microelectronic devices. However, there are many controversial issues that exist in the growth of epitaxially strained islands. Experimental results with Ge/Si(001) systems at temperatures 475,[1] 575,[2] and 603 K (Ref. 3) show that islands adopt pyramid, or hut shapes with square or elongated square bases and faceted surfaces. These islands are believed to be in a meta-stable state, which does not undergo ripening upon growth interruption.[1–3] The experimental results with Ge/Si(001) systems at 823 K (Ref. 4) show that pyramidal islands are formed first and then transform into a spherical-capped shape, called a dome. Pyramids and domes can coexist, with neither experiencing ripening. Experimental results with Ge/Si(001) systems at 923 K (Ref. 5) show that the hut islands and dome islands can coexist, however, both are unstable and undergo ripening. Experimental results with $Si_{0.8}Ge_{0.2}$/Si(001) at 1028 K (Ref. 6) show that strain-induced hut islands can strongly self organize into an almost uniform and regular squared array. Experimental results with $Si_{0.8}Ge_{0.2}$/Si(001) at 1123 K (Ref. 7) show that strain-induced islands can weakly self-organize at early stage and thereafter undergo ripening.

For the experiments with Ge/Si(001) systems, the non-ripening islands are obtained at temperatures below 603 K;[1–3] the coexisting and stable islands are obtained at 823 K;[4] and the coexisting and unstable islands are obtained at 923 K.[5] The strong self organization of islands of $Si_{0.8}Ge_{0.2}$/Si(001) occurs at 1028 K,[6] while weak the self organization of the same system occurs at 1123 K.[7] From these comparisons, our argument is that growth temperature must play an important role in the stability and self organization of epitaxial islands and the inconsistencies existing in the experimental results are due to the variation of surface energy anisotropy, which is induced by the variation of growth temperature and material composition.

Energetic analyses[8,9] show that islands can be stable, while simulation results[10–12] show that islands are unstable and undergo ripening. Each of these analyses includes strain energy relaxation as a driving force for island formation and ripening. For the unstable cases in Refs. 10, 11, and 12, they assume that surface energy is isotropic, while for the stable cases in Refs. 8 and 9, they assume that the surface energy is cusped at the wetting layer surface and edge surfaces of the islands. Kinetic simulations and energetic analyses in Ref. 13 show that the strong surface energy anisotropy and strong wetting effect can induce a stable hexagonal island array. Energetic analysis, which treats fully faceted islands with fixed facet slopes, has shown that changes of surface energy and island volume can result in the shape transition of strained islands.[14]

It is known that surface energy anisotropy can be changed by changing the material composition and temperature.[15] Two-dimensional analyses[16] have shown that, on the one hand, there is no cusp in the plot of surface energy versus orientation at finite temperature. On the other hand, if there is a cusp in the surface energy, then this singular surface will be stable against any small perturbation and it always remains flat. Since experimental results have shown surface roughening of thin films and shape transition of strained islands, it is reasonable to assume that at the temperatures used in the above experiments the surface energy is free of cusps.[16] In the previous analyses,[8–12,14] the surface energy either was assumed to be isotropic or to be cusped. Here, we will treat the surface energy as a smooth function of surface orientation.

To do the kinetic simulations of surface evolution requires the consideration of strain energy, surface energy and surface energy anisotropy. However, the exact three-dimensional surface energy form is not available. But some reasonable forms can be deduced from existing experimental results. The experimental results observed in Ref. 17 have shown that for Ge/Si systems, (001), (105), and (103) surfaces are found to be thermodynamically stable and accordingly their surface energy densities are local minima. We call these minima ''first minimum,'' ''second minimum,'' and ''third minimum,'' respectively. In the (001) plane, an anisotropy form with fourfold symmetry is assumed.

By considering above factors our three-dimensional simulations demonstrate that the change of the surface energy anisotropy can change the self organization, stability and shape transition of islands. With weak or without surface energy anisotropy, islands are unstable and undergo ripening. If the energy barrier between the second minimum and the

third minimum is high, then no island transition occurs and only square based or elongated square-based islands appear. If the energy barrier between the second minimum and the third minimum is intermediately high, then a bi-mode island distribution appears. The islands can coexist without ripening even when subjected to long-time annealing. If the energy barrier between the second minimum and the third minimum is low, then all islands evolve into the third minimum without being trapped in the second minimum. With the present simulation results, the discrepancies existing in the experimental results can be explained.

PROBLEM FORMULATIONS

We assume that the top surface of the substrate is covered with an epitaxial thin film of thickness h_f. Both thin film and substrate are modeled as isotropic, linear elastic solids with the same shear modulus G and Poisson's ratio ν, but different lattice parameters. Let a_f and a_s denote the stress-free lattice spacing of thin film and substrate, respectively. Define the mismatch strain, ε_0, as $\varepsilon_0=(a_f-a_s)/a_s$. The corresponding strain energy density, ω_0, in the planar film is given by $\omega_0=2G\varepsilon_0^2(1+\nu)/(1-\nu)$. At time $t=0$, the surface is perturbed randomly. Upon constant temperature annealing, the film surface starts to roughen and breaks up into islands.

Surface diffusion is driven by a variation of chemical potential μ, which causes atoms to migrate from regions of high-chemical potential to those of low-chemical potential. There are three contributions to the chemical potential of an atom on the surface of the thin film. The first is the energy of the surface, the second is the contribution from surface energy anisotropy, and the third is due to the elastic strain energy stored in the volume of material associated with an atom.[18] Thus,

$$\mu=\mu_0+\Omega\left(\omega-\kappa\gamma+\nabla_s\cdot\frac{\partial\gamma}{\partial\mathbf{n}}\right), \tag{1}$$

where μ_0 is the chemical potential of the bulk, Ω is atomic volume of the film, ω is the strain energy density, γ is the surface energy, which depends on surface orientation, material composition and temperature, κ is the sum of two principal curvatures, $\mathbf{n}$ is the surface normal vector, and ∇_s is the surface gradient operator. From mass conservation, the normal velocity of the surface in the reference state is

$$\nu_n=D\nabla_s^2\mu, \tag{2}$$

where $D=D_s\delta_s/kT$, D_s is the surface diffusion coefficient, δ_s is the thickness of the diffusion layer, k is the Boltzmann constant, and T is temperature. The distribution of strain energy density in the system is calculated by a finite element method.[19] A finite element method is used to solve the diffusion Eq. (2), the corresponding weak form is

$$\int_S\nu_n\delta\nu_n dA=\int_S D\Omega\nabla_s^2\left(\omega-\kappa\gamma+\nabla_s\cdot\frac{\partial\gamma}{\partial\mathbf{n}}\right)\delta\nu_n dA, \tag{3}$$

where, S is the thin film surface. By using the surface divergence theorem, assuming symmetrical boundary conditions, and neglecting the boundary term associated with $(\partial\gamma/\partial\mathbf{n})\cdot\mathbf{m}$, where $\mathbf{m}$ is the unit vector normal both to $\mathbf{n}$ and to the boundary curve, drawn outward from the surface region the above equation can be written as:

$$\int_S\nu_n\delta\nu_n dA=\int_S D\Omega\left[(\omega-\kappa\gamma)\nabla_s^2\delta\nu_n-\frac{\partial\gamma}{\partial\mathbf{n}}\cdot\nabla_s(\nabla_s^2\delta\nu_n)\right]dA. \tag{4}$$

The above equation is very stiff owing to the terms κ and $\partial\gamma/\partial\mathbf{n}$. Hence, a semi-implicit Euler scheme is used to integrate the equation. The final equation used in the calculation is

$$\begin{aligned}\int_S q\,\delta\nu_n+\Delta t\Omega D\Bigg\{\Bigg[&(\nabla_s^2q+(\kappa^2-2K)q)\gamma-\kappa\frac{\partial\gamma}{\partial\mathbf{n}}\cdot\nabla_s q\Bigg]\nabla_s^2\delta\nu_n+\Bigg\{2\frac{\partial\nabla_s q}{\partial\mathbf{n}}\cdot\frac{\partial\gamma}{\partial\mathbf{n}}-\Bigg[\Bigg(L\frac{\partial\gamma}{\partial u}\\&-M\frac{\partial\gamma}{\partial\nu}\Bigg)\frac{\partial\nabla_s q}{\partial u}+\Bigg(N\frac{\partial\gamma}{\partial\nu}-M\frac{\partial\gamma}{\partial u}\Bigg)\frac{\partial\nabla_s q}{\partial\nu}\Bigg]\Bigg/T^2\\&-2\Bigg[\Bigg(\frac{\partial\gamma}{\partial u}\frac{\partial\mathbf{n}}{\partial\nu}\cdot\frac{\partial\nabla_s q}{\partial\nu}\frac{\partial\mathbf{n}}{\partial u}+\frac{\partial\gamma}{\partial\nu}\frac{\partial\mathbf{n}}{\partial u}\cdot\frac{\partial\nabla_s q}{\partial u}\frac{\partial\mathbf{n}}{\partial\nu}\Bigg)\Bigg]\Bigg/T^2\\&-\Bigg[\Bigg(L\frac{\partial}{\partial\mathbf{n}}\frac{\partial\gamma}{\partial u}-M\frac{\partial}{\partial\mathbf{n}}\frac{\partial\gamma}{\partial\nu}\Bigg)\cdot\nabla_s q\frac{\partial\mathbf{n}}{\partial u}+\Bigg(N\frac{\partial}{\partial\mathbf{n}}\frac{\partial\gamma}{\partial\nu}\\&-M\frac{\partial}{\partial\mathbf{n}}\frac{\partial\gamma}{\partial u}\Bigg)\cdot\nabla_s q\frac{\partial\mathbf{n}}{\partial\nu}\Bigg]\Bigg/T^2+\Bigg(\frac{\partial\gamma}{\partial u}\frac{\partial\mathbf{n}}{\partial\nu}+\frac{\partial\gamma}{\partial\nu}\frac{\partial\mathbf{n}}{\partial u}\Bigg)\\&\times\Bigg(\frac{\partial\nabla_s q}{\partial\nu}\cdot\frac{\partial\mathbf{n}}{\partial u}+\frac{\partial\nabla_s q}{\partial u}\cdot\frac{\partial\mathbf{n}}{\partial\nu}\Bigg)\Bigg/T^2\Bigg\}\cdot\nabla_s(\nabla_s^2\delta\nu_n)\Bigg\}dA\\&=\int_S\Delta tD\Omega\left[(\omega-\kappa\gamma)\nabla_s^2\delta\nu_n-\frac{\partial\gamma}{\partial\mathbf{n}}\cdot\nabla_s(\nabla_s^2\delta\nu_n)\right]dA,\end{aligned} \tag{5}$$

where, u,ν are curvilinear coordinates of the film surface, $q=\Delta t\nu_n,\Delta t$ is the time step, $L=\partial\mathbf{n}/\partial u\cdot\partial\mathbf{n}/\partial u$, $M=\partial\mathbf{n}/\partial u\cdot\partial\mathbf{n}/\partial\nu$, $N=\partial\mathbf{n}/\partial\nu\cdot\partial\mathbf{n}/\partial\nu$, $T^2=LN-M^2$. A higher-order finite element is used to solve the above equation.[12,19]

The abrupt discontinuity in mismatch strain at the film/substrate interface causes some numerical difficulties. We have therefore followed Kukta and Freund,[10] and regularized the problem by introducing a transition region of thickness h_w between the substrate and the thin film. The mismatch strain is assumed to vary linearly between ε_0 at the top of the transition layer to zero at the bottom. We have found that our numerical results are insensitive to the choice of strain variation and transition layer thickness.[12] The reason for this lack of sensitivity is that the volume of material removed from the transition layer during surface roughening and island formation is negligible even if we use a relatively thick transition layer ($h_f=h_w$).

We have assumed that the surface energy is a smooth function of surface orientation and its anisotropy is of four-fold symmetry in the (001) plane surface. Accordingly the function form for the surface energy is chosen as

$$\gamma(\theta,\phi)=\gamma_0\{1+f(\theta)[\eta-\cos(4\phi)]\}, \tag{6}$$

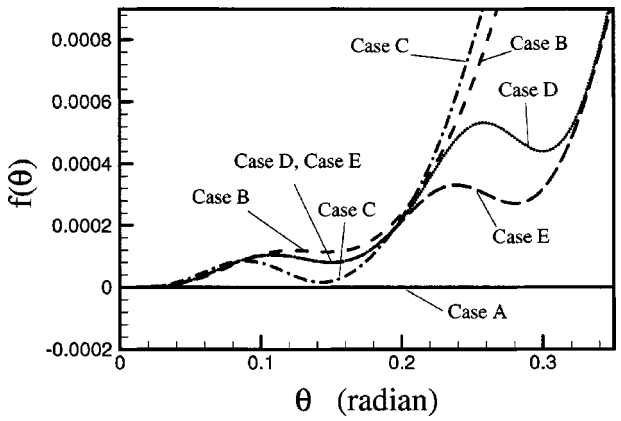

FIG. 1. The plot depicts the variation of the function $f(\theta)$ in Eq. (6) with θ for different simulation cases.

where θ is the angle between **n** and [001], ϕ is the angle between the projection of **n** on (001) and [100], γ_0 is the surface energy on (001) surface, the function $f(\theta)$ and parameter η are used to describe the surface energy anisotropy. $f(\theta)$ is chosen to be minimum near (001), (105), and (103) surfaces except in the isotropic case. The different forms of $f(\theta)$ used in the present simulations are shown in Fig. 1. Case *A* is the isotropic case. Case *B* has a shallow second minimum and a high barrier between the second minimum and the third minimum (beyond the limit of the figure). Case *C* has a deep second minimum and a high barrier between the second minimum and the third minimum (beyond the limit of the figure). Case *D* has an intermediately high barrier between the second minimum and the third minimum. Case *E* has a low-barrier between the second minimum and the third minimum. In all our simulations, η is chosen to be 1.5. All simulations start from a same initially random surface.

The present results are normalized as $\omega_* = \omega/\omega_0$, $l_* = l\omega_0/\gamma_0$, $t_* = t\gamma_0\Omega D(\omega_0/\gamma_0)^4$, where, l is length scale, t is time scale, ω_0 and γ_0 are the strain energy density and the surface energy density at the initially perfectly flat thin film surface, respectively. In the calculations, the length and width of the simulation cell are chosen as $X_* = 24$, $Y_* = 24$, respectively; $h_{f*} = 0.1$; and $h_{w*} = 0.1$. The finite element nodes on the film surface form an array of 65×65 points.

RESULTS AND DISCUSSIONS

It should be noted that the relative amount of surface energy change is very small, however such a small variation of surface energy can cause a significant difference in island evolution. The results of Case *A* are shown in Fig. 2. It can be seen that at the early stages, Fig. 2(a), the island array can self organize, but thereafter ripening occurs, Fig. 2(b). Islands with different size and aspect ratio can be observed. The results of Case *B* are shown in Fig. 3. It can be seen that after the surface breaks up into islands, Fig. 3(a), the islands start to self organize, Fig. 3(b). These islands are stable and do not undergo ripening even subject to long-time annealing. The final configuration of these islands shown in Fig. 3(b) is a square array which shows remarkably uniformity and regularity. Also these islands have a square base and their edge

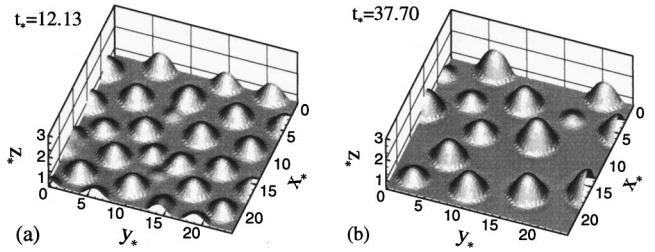

FIG. 2. The evolution of islands for Case *A* (the isotropic case); (a) $t_* = 12.13$, (b) $t_* = 37.70$. At the initial stages, islands self organize into a relative uniform and regular array, thereafter ripening occurs.

surfaces are slightly faceted. Large islands have an elongated base while small islands have a square base. The results of Case *C* are shown in Fig. 4. It can be seen that after islands are formed, Fig. 4(a), they start to evolve and coalesce, and finally reach a state which does not undergo ripening, Fig. 4(b). Larger islands adopt an elongated base, while smaller islands adopt a square base. The results of Case *D* are shown in Fig. 5. Islands with square or elongated bases appear first, Fig. 5(a), thereafter, a bimode distribution of islands can be clearly seen, Fig. 5(b). The smaller islands with lower aspect ratios do not disappear even when subjected to long-time annealing.[20] The results of Case *E* are shown in Fig. 6. During the late stages, only a unimode distribution of islands with higher aspect ratio appear, which corresponds to the third minimum. This clearly shows that in this case the second minimum does not trap any islands.

From our results, we can see that the surface energy anisotropy determines the self-organization, shape transition and stability of epitaxial islands. We are very encouraged when comparing the present results with experimental results. The results of Case *A* are similar to the experimental results conducted at very high temperature by Ozkan *et al.*[7] This is because at very high temperature, the surface energy density is nearly isotropic. Case *B* shows a remarkable island array with good regularity and uniformity. It suggests that if one can choose the surface energy anisotropy by tailoring the material's composition and/or by changing the annealing temperature, then a uniform and regular island array can be achieved. This result shows remarkable similarity to the experimental results of Floro *et al.*[6] Case *C* shows a resemblance to the experimental results of Mo *et al.*,[1] Kastner and Voigtlander[2] and Steinfort *et al.*[3] In their observations, they found that large hut islands have an elongated shape while small huts have a square based shape. The elongated islands

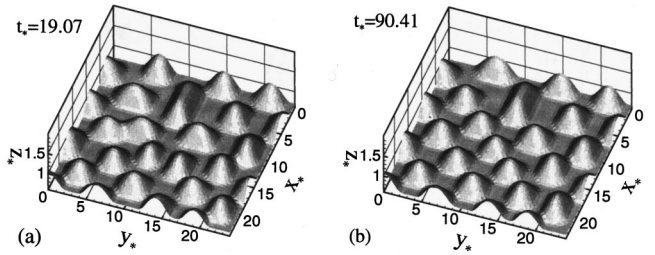

FIG. 3. The evolution of islands for Case *B*; (a) $t_* = 19.07$, (b) $t_* = 90.41$. The islands are able to self-organize into an almost uniform and regular squared array and do not undergo ripening.

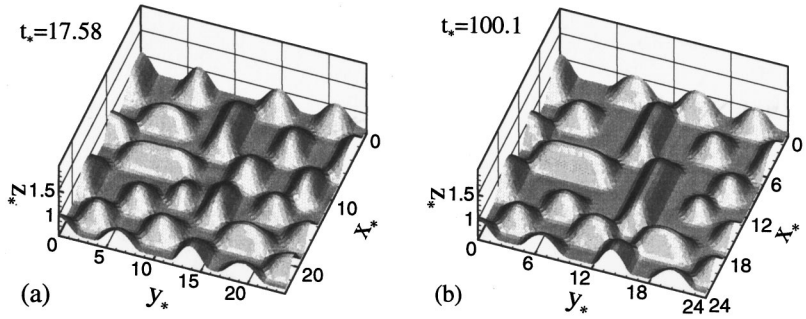

FIG. 4. The evolution of islands for Case *C*; (a) $t_*=17.58$, (b) $t_*=100.1$. The islands evolve into a state, which does not undergo ripening. These islands are not uniform and regular.

are oriented in the ⟨001⟩ direction. These observations are in good agreement with Case *C*. Hut islands and dome islands were observed to coexist by Medeiros-Ribeiro *et al.*[4] and Ross, Tersoff, and Tromp.[5] Medeiros-Ribeiro *et al.* found that there was state in which neither group of islands experienced ripening. This picture is consistent with the results of Case *D* shown in Fig. 5(b). Ross, Tersoff, and Tromp found the two groups of islands were unstable and underwent ripening. The group of smaller islands eventually disappeared. Since they used growth method, islands had to be nucleated first as huts. After growing large, the huts would transform into domes. While the present simulation uses controlled annealing. During the annealing, the islands are formed as a mixture of huts and domes at first, and eventually all become domes. Therefore the experimental results of Ross, Tersoff, and Tromp are consistent with the picture of Case *E*. Since in this case there is a high barrier beyond the third minimum as shown in Fig. 1, the ripening of the high aspect islands is suppressed. The subtle difference between the two experiments is in the growth temperature, which is 100 K different. We can see that the change of surface energy between Case *D* and Case *E* is very small, but the island evolution is quite different. It is reasonable to believe that such a small change of surface energy results from the temperature difference and the difference in the two experiments results from the growth condition.

It is well known that strain energy relaxation arising from the interaction among the islands is a driving force for surface roughening, while the surface energy is a stabilizing force working against surface roughening. When a minimum exists in the surface energy, then the surface energy anisotropy provides an additional stabilizing force against surface roughening.[16] From the present simulations, it can be seen that the high surface energy barrier between minima is crucial for the island stability; the lower surface energy barrier between minima is crucial for island shape transition; and the depth of the surface energy minima is crucial for island self organization. For strongly self-organized and stable islands, a shallow second minimum and a high barrier between the second minimum and the third minimum of surface energy are required. It should be noted that the non-ripening states in the present simulations are all in a meta-stable state. Obviously, if temperature is increased, the anisotropy will become weak and islands will undergo ripening.

It has been shown that large faceted islands have an elongated shape and small faceted islands have a square-based shape.[21] This conclusion is in agreement with the present results when all islands are trapped in the second minimum. But it seems that there is another degree of freedom, which also controls island shape: the depth of the second minimum. Our simulations show that the deeper the second minimum, the more likely the islands will have an elongated base. Many experiments[1–3] have shown that the lower the temperature the more elongated the island bases. This is consistent with the present results. But when the islands are trapped in the third minimum, although a fourfold symmetry is applied to the in-plane anisotropy, the islands still adopt a dome shape. Hence, the islands with high aspect ratio prefer a dome shape to an elongated hut shape.

The simulations by considering strain energy and surface energy were also carried out by Chiu.[13] In his results, the initial rough surface developed into a stable hexagonal island array, each island in the array adopted a conical shape and its aspect ratio was lower than 0.01, and no island shape transition was observed. The above results are the direct conse-

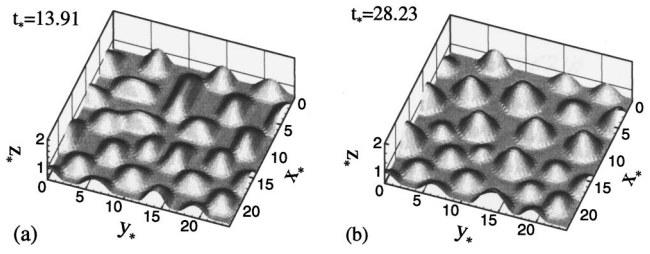

FIG. 5. The evolution of islands for Case *D*; (a) $t_*=13.91$, (b) $t_*=28.23$. The islands with squared bases are formed first, thereafter develop into a bimode distribution of islands. Even when subjected to long-time annealing, the group of smaller aspect ratio islands does not disappear.

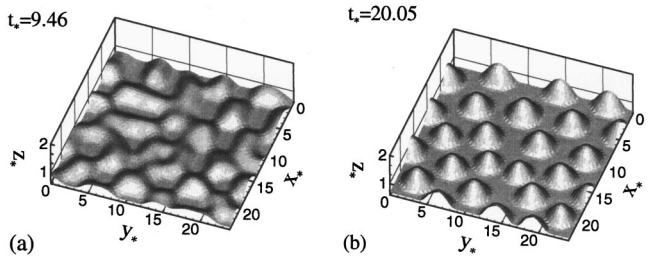

FIG. 6. The evolution of islands for Case *E*; (a) $t_*=9.46$, (b) $t_*=20.05$. The islands with squared bases are formed first, thereafter all islands are able to evolve into a unimode distribution with domed shapes.

quence of his assumption on the form of surface energy anisotropy. The conical island shape was caused by the assumption of axisymmetric surface energy, the extremely low-aspect ratio was caused by the extremely strong surface energy anisotropy, and the lack of shape transition was caused by the assumption that only one minimum was allowed in the surface energy form. Hence, the differences between the present results and the results in Ref. 13 are mainly due to the choice of different surface energy form.

The shape transition of epitaxial islands was also studied by Daruka *et al.*[14] by using energetic analysis. In their analysis, the surfaces were treated to be fully faceted with fixed face slopes and no interaction among the islands was taken into account. Their results showed that the island volume and the relative values of surface energy on the wetting surface and island side surfaces determined the island transition. However, the present simulation results have shown that the relative values of surface energy levels are not so important for the island shape transition. In fact, it is the barriers between the surface energy levels that control the transition of island shape.

CONCLUSIONS

Three-dimensional computer simulations have been conducted to simulate the island formation during controlled annealing. It is shown that the surface energy anisotropy, which may be changed by the change in material composition and temperature, plays an important role in the self-organization, island shape transition, and stability of epitaxial islands. With the present results, the inconsistencies existing in the experiments can be explained. More importantly we have demonstrated that if we can choose certain surface energy anisotropies by tailoring the material composition and/or by changing the annealing temperature, then strongly self-organized and nonripening island arrays may be obtained.

ACKNOWLEDGMENTS

The author thanks Dr. C. H. Chiu for helpful discussions and Dr. P. M. Moran for reviewing the manuscript.

*Electronic address: yw-zhang@imre.org.sg

[1] Y.-W. Mo, D. E. Savage, B. S. Swartzentruber, and M. G. Lagally, Phys. Rev. Lett. **65**, 1020 (1990).
[2] M. Kastner and B. Voigtlander, Phys. Rev. Lett. **82**, 2745 (1999).
[3] A. J. Steinfort, P. M. L. O. Scholte, A. Ettema, F. Tuinstra, M. Nielsen, E. Landemark, D. M. Smiligies, R. Feidenhans, G. Falkenberg, L. Seehofer, and R. L. Johnson, Phys. Rev. Lett. **77**, 2009 (1996).
[4] G. Medeiros-Ribeiro, A. M. Bratkovski, T. I. Kamins, D. A. A. Ohlberg, and R. S. Williams, Science **279**, 353 (1998).
[5] F. M. Ross, J. Tersoff, and R. M. Tromp, Phys. Rev. Lett. **80**, 984 (1998).
[6] J. A. Floro, E. Chason, M. B. Sinclair, L. B. Freund, and G. A. Lucadamo, Appl. Phys. Lett. **73**, 951 (1998).
[7] C. S. Ozkan, W. D. Nix, and H. Gao, Appl. Phys. Lett. **70**, 2247 (1997).
[8] V. A. Schchukin, N. N. Ledentsov, P. S. Pop'ev, and D. Bimberg, Phys. Rev. Lett. **75**, 2968 (1995).
[9] I. Daruka and A.-L. Barabasi, Phys. Rev. Lett. **79**, 3708 (1997).
[10] R. V. Kukta and L. B. Freund, J. Mech. Phys. Solids **45**, 1835 (1997).
[11] B. J. Spencer and J. Tersoff, Phys. Rev. Lett. **79**, 4858 (1997).
[12] Y. W. Zhang and A. L. Bower, J. Mech. Phys. Solids **47**, 2273 (1999).
[13] C. H. Chiu (unpublished).
[14] I. Daruka, J. Tersoff and A.-L. Barabasi, Phys. Rev. Lett. **82**, 2753 (1999).
[15] C. Rottman and M. Wortis, Phys. Rev. B **24**, 6274 (1981).
[16] Y. W. Zhang, Phys. Rev. B **60**, 13325 (1999).
[17] Z. Gai, R. G. Zhao, H. Ji, X. Li, and W. S. Yang, Phys. Rev. B **56**, 12 308 (1997).
[18] P. H. Leo and R. F. Sekerka, Acta Metall. **37**, 3119 (1989).
[19] Y. W. Zhang, A. L. Bower, L. Xia, and C. F. Shih, J. Mech. Phys. Solids **47**, 173 (1999).
[20] Due to the small size of some of the smaller islands, the finite element meshes are not able to resolve the squared base well. But the difference in aspect ratio for two groups of islands can be clearly seen.
[21] J. Tersoff and R. M. Tromp, Phys. Rev. Lett. **70**, 2782 (1993).